

ASSESSING CONDITION OF TURBINE ENGINE CERAMIC COMPONENTS THROUGH NDE TECHNOLOGY*

W. A. Ellingson, J. G. Sun, C. Deemer, S. Erdman, and C. Prested
Argonne National Laboratory
Argonne, IL 60439

January 2002

The submitted manuscript has been created by the University of Chicago as Operator of Argonne National Laboratory (Argonne) under Contract No. W-31-109-ENG-38 with the U.S. Department of Energy. The U.S. Government retains for itself, and others acting on its behalf, a paid-up, nonexclusive, irrevocable worldwide license in said article to reproduce, prepare derivative works, distribute copies to the public, and perform publicly and display publicly, by or on behalf of the Government.

Distribution

R. B. Poeppel, ET/212
D. Schmalzer, OTD/201
W. Shack, ET/212
R. Valentin, ET/308
A. C. Raptis, ET/308

Invited paper presented at the International Conference on Advances in Life Assessment and Optimization of Fossil Power Plants, March 11-13, 2002, Orlando, FL.

*Work supported by the U.S. Department of Energy, Office of Energy Efficiency and Renewable Energy/Office of Power Technology program, under Contract W-31-109-Eng-38

ASSESSING CONDITION OF TURBINE ENGINE CERAMIC COMPONENTS THROUGH NDE TECHNOLOGY*

W. A. Ellingson, J. G. Sun, C. Deemer, S. Erdman, and C. Prested
Energy Technology Division
Argonne National Laboratory
Argonne, IL 60439

Abstract

Thermal barrier coatings (TBCs) and environmental barrier coatings (EBCs) are under development for hot-gas path components to allow higher gas-firing temperatures in advanced (high-efficiency, low-emission) gas turbines. Increasing dependence on the reliability of TBC and EBC components has driven the need for nondestructive evaluation (NDE) methods to assess the condition, or “health status,” of these coatings. NDE methods based on elastic optical scatter and thermal imaging have been applied to TBC-coated test specimens that were thermally cycled and to EBC-coated SiC/SiC components that were run in 4.5 MW(e) field-test turbines. One primary interest is to develop NDE methods that can predict a prespall condition. Resulting data suggest a correlation between laser scatter data and thermal cycles for TBC-coated specimens, and thermal imaging results have demonstrated prespall detection for an EBC-coated SiC/SiC combustor liner.

Introduction

Significant advances have been made in the development and understanding of high-temperature ceramic TBCs used to protect blades, vanes, and combustor liners for gas turbines (1-3). Usually composed of yttria-stabilized zirconia (YSZ), these coatings protect the metal substrates from the high-temperature gas stream. As the gas-path temperature is pushed to higher temperatures, and as reliance on these coatings remaining intact increases, their failure becomes a major concern. Thus, development of NDE technologies that can provide information on the TBC condition is a high priority.

Recently, ceramic matrix composites, most commonly melt-infiltrated (MI) SiC/SiC, have been under development for lining the combustion chamber in low-emission turbines with high gas firing temperatures. These composites have been shown to have unacceptable recession rates if not coated with an EBC (4). Oxide-based composites are also under development, but these will not be discussed in this paper. Current EBCs for SiC/SiC are composed of barium-strontium alumino-silicate (BSAS) and are applied by plasma spray methods (4). Because these coatings are also necessary for continued safe operation of the turbine, NDE technologies that can assess the EBC condition are necessary.

Several NDE methods are under development for estimating the condition of TBC and EBC coatings. These NDE methods include thermal imaging, air-coupled ultrasound, X-ray computed tomography, and optical scattering using low power lasers. The sections below provide brief

descriptions of two of the NDE methods under development, followed by tests of these methods with TBC- and EBC-coated samples.

Description of NDE Test Methods

Laser Back-Scatter Method

The polarized back-scattered laser NDE method (see Fig. 1) is based on a modification of the reflectometry method (5). This backscatter method utilizes two detectors. After the polarized laser light is incident on the test specimen, the backscattered light, which penetrates through the optically translucent coatings and then reflects back off the interface, and is received by the two detectors. In front of the first detector is a highly polished first-surface mirror that has a small-diameter aperture, thereby only allowing light that is back-scattered over a narrow angle to be detected, while the second detector has no aperture and, therefore, detects light scattered back over a much larger angle. On the basis of the voltage output from these two detectors, various features related the scatter pattern can be discriminated with special computer software. Laser scatter data for an entire test are acquired by raster scanning the sample under computer control. Because shapes associated with turbine engine vanes and blades are complex, it would not be possible to keep the laser light with normal incidence without the use of a computer-controlled 6-axis robot. In our case, we have installed a robot arm that allows import of a computer-aided design (CAD) file of the materials under study. The software package allows development of a raster scan pattern for that material.

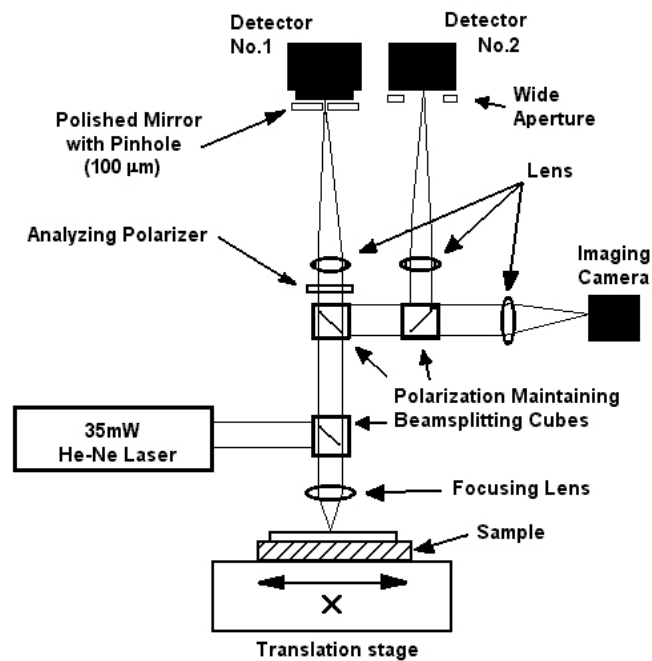


Fig. 1. Schematic diagram of polarized back-scatter laser NDE method.

Thermal Imaging Method

The thermal imaging method is based on detection of the time-dependent surface temperature after there has been thermal stimulation (6-8). We use two modes of operation: (1) transmission, where the thermal stimulation is placed on one side of the test sample and the detector on the opposite side, and (2) one-sided, where the thermal stimulation and the detector are both placed on the same side of the test specimen. This NDE method has been under development for several years and has been fully described (6-8). Figure 2 is a schematic diagram of the one-sided thermal imaging arrangement. The high-frame-rate infrared camera utilizes a focal plane array with 3- to 5- μm band pass. The flash lamps are operated by a 6.4-kJ power supply. Spectral output of the flash can be customized through use of different gases in the flash tube, as well as various external filters.

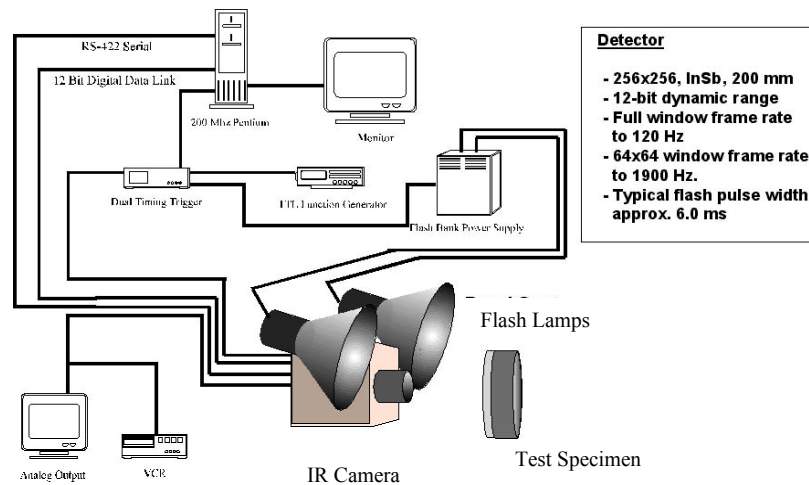


Fig. 2. Schematic diagram of one-sided infrared thermal imaging NDE system.

Materials Tested

TBC Specimens

While our efforts have involved many TBC-coated components, this discussion will be limited to two types of sample.

The first type (see Fig. 3), prepared by the University of California-Santa Barbara, was a 25-mm-diameter specimen made with René N5 substrate coated with 7 wt. % YSZ applied using electron beam-physical vapor deposition (EB-PVD), but having no bond coat. A single sample was prepared such that intentional debonds of the TBC were introduced through use of a high-power CO₂ laser. Before being studied by the two NDE methods, the sample was subjected to low-temperature, steady-state heating on the uncoated side, while the steady-state surface temperature on the coated side was observed by thermal imaging. The initial 1.55-J pulse applied to the center of the sample was so intense that it caused the TBC to spall off, as seen in the center-damaged region of Fig. 3c. The subsequent power levels applied were 140, 100, 75, and 50 mJ. This sample was then studied by the two NDE methods.

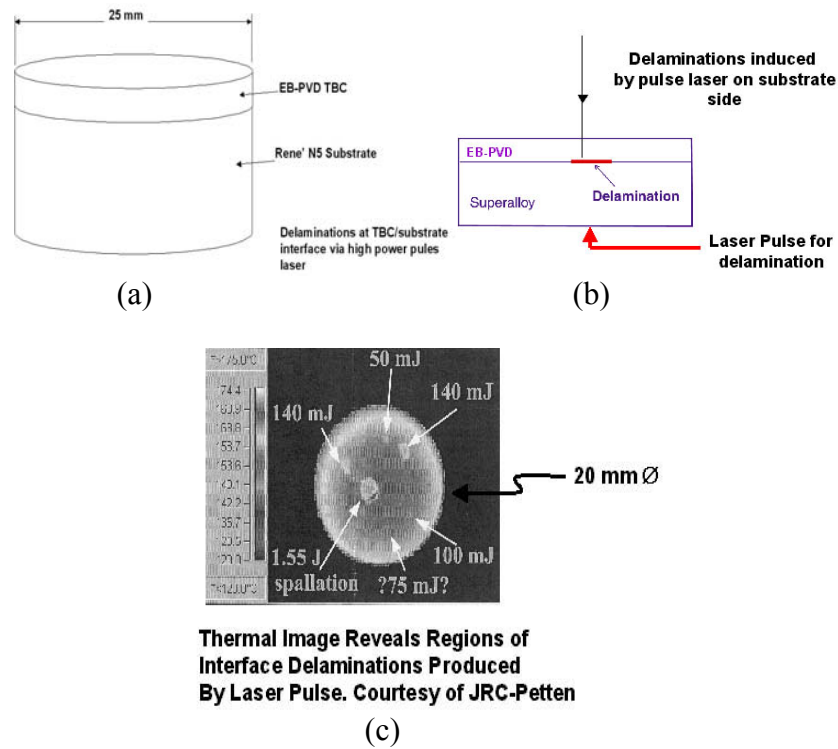


Fig. 3. EB-PVD test sample used for initial NDE studies: (a) schematic diagram of sample, (b) schematic diagram showing test setup for generation of debonds, and (c) steady-state thermal image showing locations of debonds.

The second type was a 25-mm-diameter button sample made with CMSX-4 substrate, plasma-sprayed MCrAlY bond coat, and a 7YSZ TBC applied by EB-PVD. Three such samples, all produced by the University of Connecticut at the same time, were heat-treated through exposure to numbers of thermal cycles. Sample GEP had no thermal cycles, sample GEP-9 had 5 thermal cycles, and sample GEP-70 had 70 thermal cycles. The thermal cycles involved raising the temperature to 1121°C, then holding at that temperature for one hour, then decreasing to room temperature.

EBC-Coated SiC/SiC specimens

We also examined many different EBC-coated test specimens. However, only two types will be discussed here. The first type was specially prepared by United Technology Research Center (UTRC) and consisted of plasma-sprayed BSAS on an eight-ply 2D layup MI SiC/SiC. These samples were made with intentional delaminations at the various interfaces on the EBC material system (see Fig. 4). Note that the delaminations were intended to be at the interfaces (a) between the EBC and the intermediate layer, (b) between the intermediate layer and the SiC layer, and (c) between the SiC layer and the substrate. Other similar test samples were made with known porosity variations within the different layers as well, but this paper will discuss the delamination samples only. The second type of sample was full-size combustor liners consisting of an outer liner that is 76.2 cm in diameter with the EBC on the inside surface and a smaller inner liner that is 33 cm in diameter with the EBC on the outer surface. A photograph of a typical liner set is shown in Fig. 5. These liners have been discussed in detail in a recent publication (9).

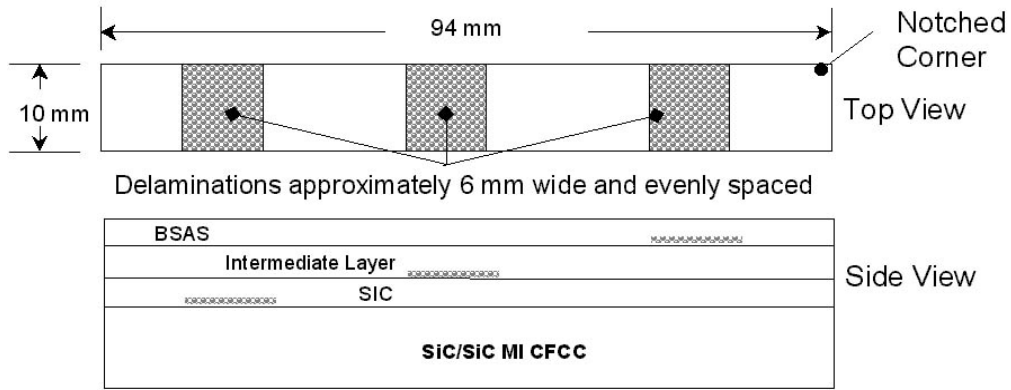


Fig. 4. Schematic diagram of EBC-coated MI SiC/SiC delamination specimen used for NDE studies (CFCC = continuous fiber-reinforced ceramic composites).

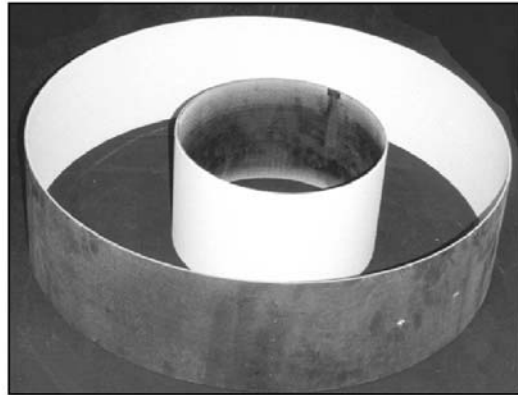


Fig. 5. Photograph of EBC-coated SiC/SiC combustor liner set. Outer liner is 76 mm in diameter, and the inner liner is 33 cm in diameter.

Results and Discussion

TBC

The sample prepared by the University of California-Santa Barbara was analyzed by both the back-scattered laser method and the one-sided thermal imaging method. Figure 6 shows the results of raster scanning for 10- μm step sizes. Several interesting features are worth noting. First, there had been a question about the existence of a debond caused by the 75-mJ pulse. The laser back-scatter method clearly shows a debond at this pulse location. Second, islands appear within each debond location, where the degree of disbond varies. This property is understandable because it is not likely that any disbonded region would be uniform over the entire area. Further, near the 1.55-J pulse, the NDE data suggest a region that is debonded but not yet spalled. The backscatter method not only shows these debond regions but suggests the extent in size as well. This method is also very fast, with the scan time for the entire image being less than 5 min.

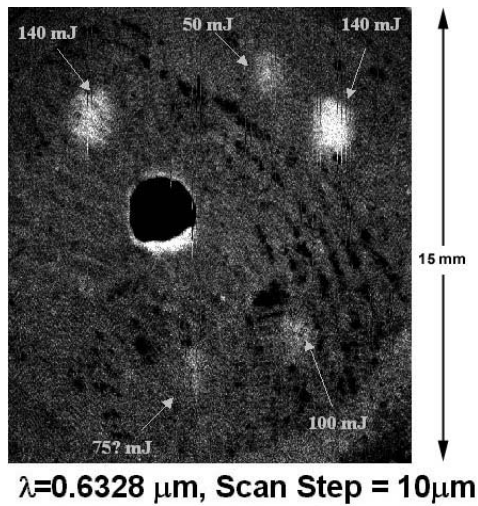


Fig. 6. Polarized back-scattered light data from debond EB-PVD sample shown in Fig. 3.

The same sample was analyzed by the one-sided thermal method. By capturing a single infrared camera frame at some specified time after the stimulation flash, regions that are debonded will have a slower cooling curve than bonded regions. Thus, at some optimal time after the thermal stimulation pulse, there will be a maximum “difference” temperature. Figure 7 shows a single infrared image frame captured 0.2 s after the thermal pulse was applied. This thermal image data reveal several features that correlate with the back-scattered laser data. First is the comparison between the two 140-mJ pulse debonds. The thermal data corroborate the laser data in that these two locations do not appear to be debonded equally. Second, the debond caused by the 50-mJ pulse appears to be more severe than the 75-mJ debond that was detected by the laser scatter. Note that the 75-mJ debond region is not detected by the one-sided thermal image data.

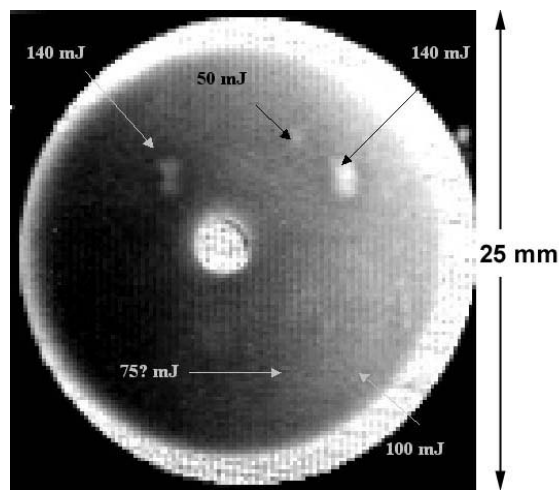


Fig. 7. One-sided thermal image of 25-mm debonded EB-PVD sample shown in Fig. 3.

The samples prepared by the University of Connecticut were analyzed by the laser scatter method alone. The resulting scatter images are shown in Fig. 8. Note the difference in the “black spots” which appear in the scan data. These scans were taken using 25- μm scan steps and represent a fairly large region. These scan data are interesting because the spallation of an EB-PVD coating usually occurs at the interface between the thermally grown oxide (TGO) layer and the bond coat (3). For prespallation detection, it would be desirable to establish an NDE parameter that could track changes at the failure site –in this case the TGO/bond coat interface. For EB-PVD coatings, one mechanism thought to be a precursor to spallation is a change in the surface topography at the TGO/bond coat interface. The optical photomicrographs of the TGO/bond coat interface in Fig. 9 suggest a certain periodicity at this interface, as well as deeper penetration depths as a function of the number of thermal cycles. It is possible that the “black spots” in the scattered light NDE data are directly related to the topology of the TGO/bond coat surface. If a correlation could be established among a prespallation stress condition, the topology of the TGO/bond coat interface, and the data from the laser scatter method, then the scattered laser light NDE method with digital image processing could be used in predicting the onset of spallation.

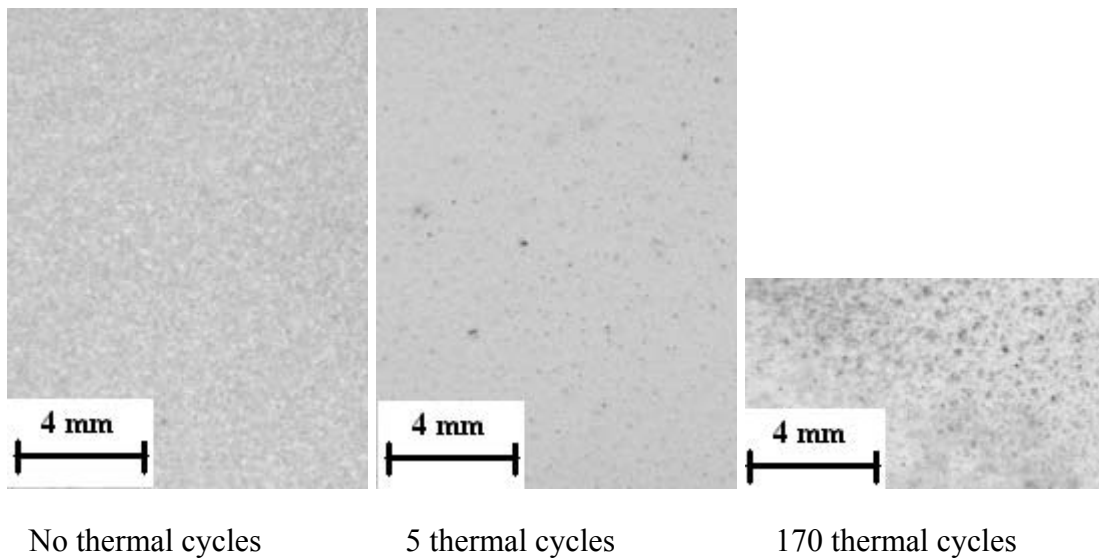


Fig. 8. Polarized back-scatter NDE data obtained from EB-PVD TBC samples subjected to thermal cycles at 1121° C.

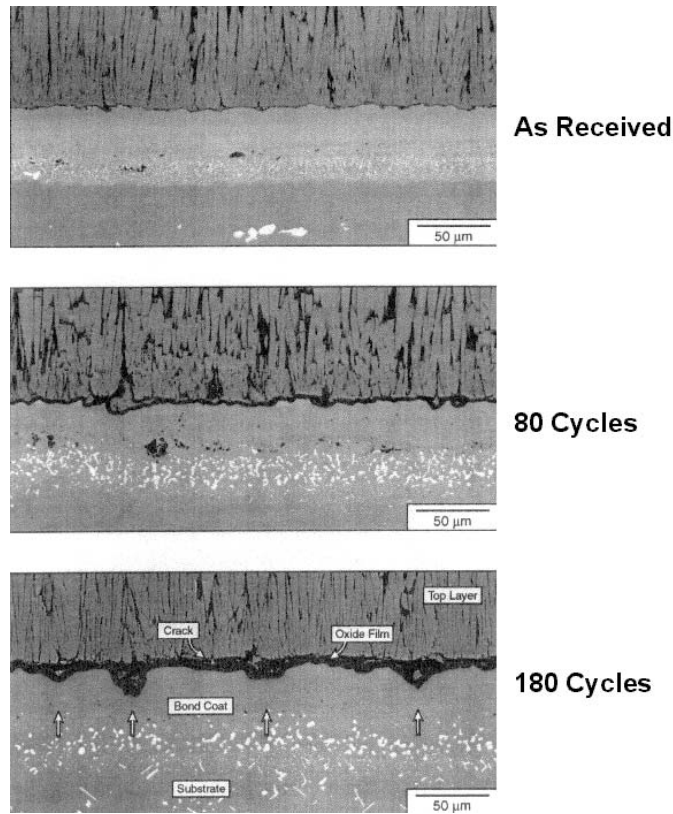


Fig. 9. Optical photomicrographs of the TGO/bond coat interface for EB-PVD TBC samples subjected to thermal cycles.

EBC

Before conducting the NDE studies of the EBC-coated SiC/SiC, the optical transmission properties of a section of free-standing BSAS were determined. Figure 10 shows the optical transmission characteristics for the BSAS EBC and an intermediate layer, which is predominantly mullite. In addition, this figure shows the output spectral characteristics of the thermal flash system. This figure demonstrates that the BSAS EBC appears nominally opaque to the spectral flash system; therefore, the thermal pulse is nearly a step input heating. Time-temperature surface images of the intentional delaminated samples, acquired at 0.1-s intervals, are shown in Fig. 11a. By establishing the time-temperature behavior for the thermal image regions above each of the seeded delaminated regions, one can estimate the depth of delaminations. Figure 11b shows the resulting time-temperature plot. The method used to estimate delamination depth is described more thoroughly in Ref. 10.

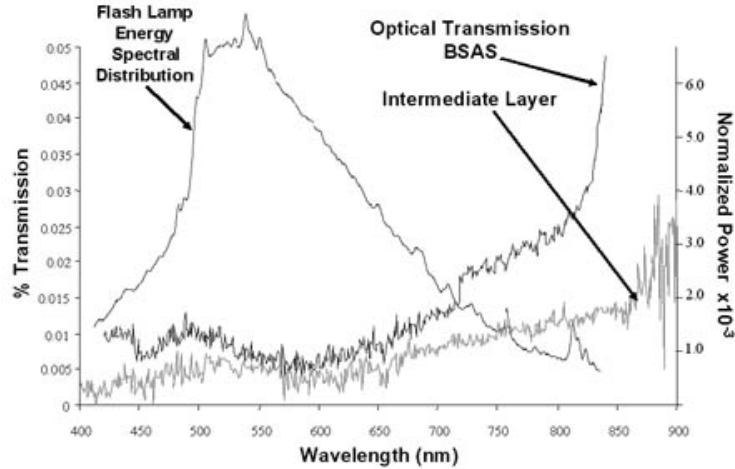
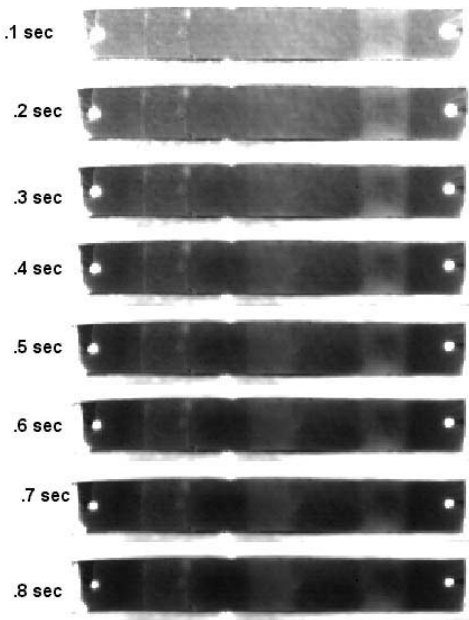
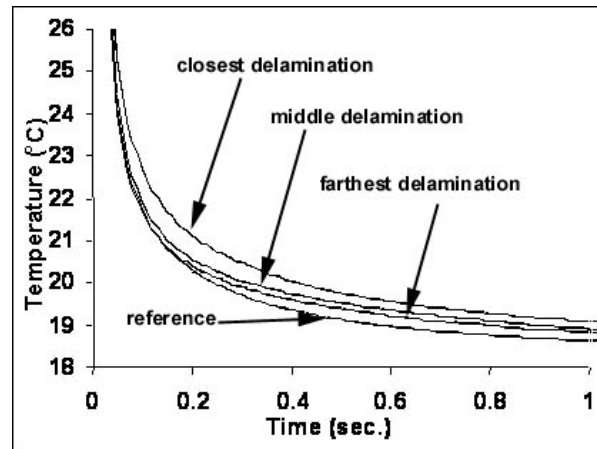


Fig. 10. Optical transmission characteristics of free-standing BSAS EBC, free-standing intermediate bond layer, and spectral output of thermal flash.



(a)



(b)

Fig. 11. Time-temperature surface images for EBC-Coated MI SiC/SiC delamination coupon shown in Fig. 4. Data obtained using one-sided thermal imaging: (a) sequence of thermal images and (b) graph of the various regions on the time-temperature image sequence.

The EBC-coated combustor liners were installed in a Solar Turbines Centaur 50 gas turbine, which is a 4.5 MWe engine. This engine and the test program have been extensively described previously (9,11,12). Prior to insertion into the engine, the EBC-coated liner was examined by through-transmission infrared imaging for uniformity. The resulting image data (see Fig. 12a)

suggest that delamination regions are likely at various locations around the liner. The depth of the delaminations is not known.

After the engine had been run, boroscope examinations of the EBC-coated liner were conducted. Figures 12b and c show the boroscope images taken after 357 hours and 1573 hours. Note that the delamination occurred at the position predicted by the NDE data, and further that the size of the delaminated region grew to include the small region adjacent that was detected in the initial NDE data.

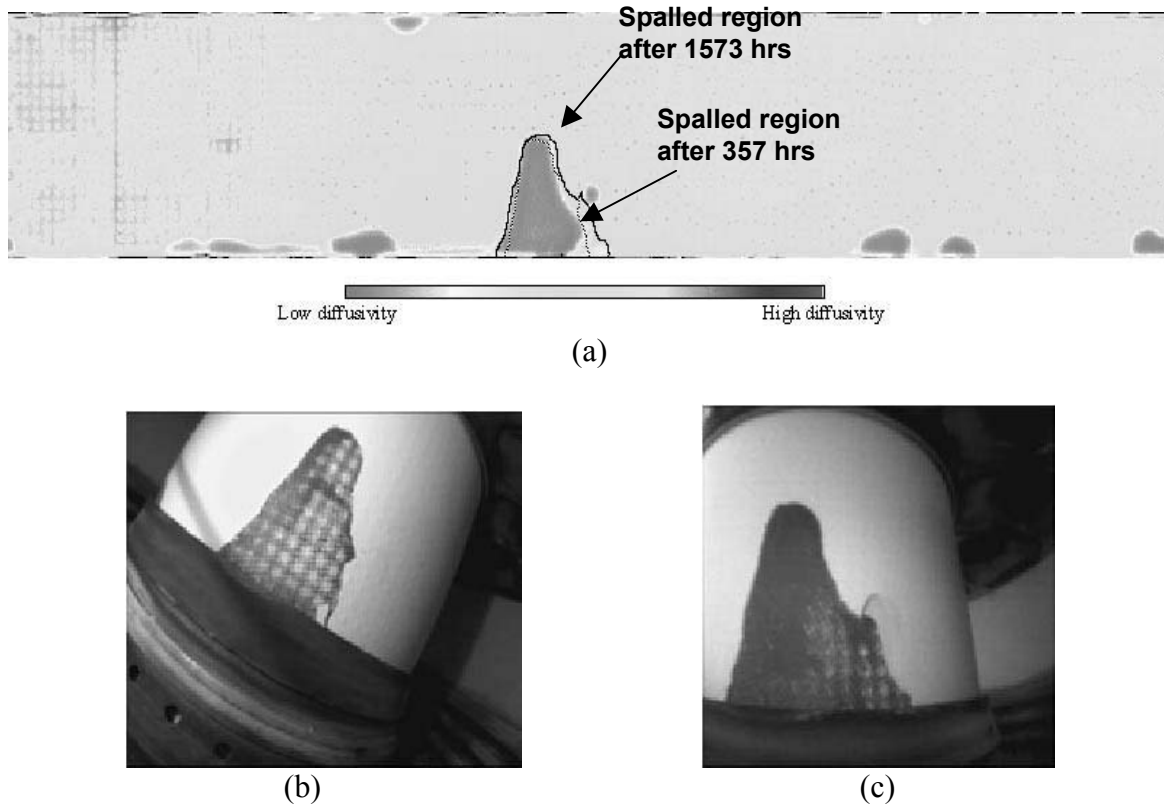


Fig. 12. Detection of Pre-spall of EBC-coated MI SiC/SiC combustor liner. Figures show (a) Infrared image of 33-cm-diameter inner liner prior to insertion into engine, (b) boroscope image of the liner after 357 hours, and (c) boroscope image of the liner after 1573 hours.

Conclusions

NDE methods are under development for TBC-coatings as well as EBC-coated composite ceramics. Initial test results have shown that changes in NDE data suggest a correlation with the number of thermal cycles in EB-PVD TBCs. However, data are currently insufficient to correlate the NDE results to any quantifiable pre-spallation condition such that predictions can be made. If the mechanism for spallation continues to support the theory wherein the TGO/bond coat interface undergoes a significant morphology change, then this might provide a recognizable feature for making quantifiable predictions from NDE data. Spectrally tuned thermal imaging

was able to detect prespallation regions for EBCs on SiC/SiC composites. The potential spall locations predicted by the NDE data were verified in field engine tests.

Acknowledgments

The authors acknowledge the many university and industrial partners who are participating in this project. For the TBC efforts, these include the University of California-Santa-Barbara, the University of Connecticut, Northwestern University (for help with determining optical transmission characteristics), and Praxair Corporation. For the EBC efforts, these include Solar Turbines and United Technologies Research Center. Clearly, such an extensive effort could not be possible without these cooperative efforts. The authors want to also fully recognize the continuing support of our sponsor, the U.S. DOE/Office of Energy Efficiency and Renewable Energy/Office of Power Technologies, under contract W-31-109-Eng-38.

References

1. North Atlantic Treaty Organization. *Thermal Barrier Coatings*. AGARD-R-823, Neuilly-Sur-Seine, France: Advisory Group for Aerospace Research and Development, AGARD, April 1998. AGARD-R-823.
2. U.S. National Research Council, National Materials Advisory Board. *Coatings for High Temperature Structural Materials*. Washington, DC: National Academy Press, 1996.
3. U.S. National Aeronautics and Space Administration. *Thermal Barrier Coating Workshop*. NASA Conference Publication 3312, 1995.
4. H. E. Eaton, G. Linsey, E. Sun, K. L. More, J. Kimmel, J. Price, and N. Miriyala. "EBC Protection of SiC/SiC Composites in the Gas Turbine Combustion Environment: Continuing Evaluation and Refurbishment Considerations." Am. Soc. of Mech. Eng., Paper No. ASME 2001-GT-513 (2001).
5. H. G. Tompkins, and W. A. McGahan. "Spectroscopic Ellipsometry and Reflectometry." New York: J. Wiley and Sons, Inc., 1999.
6. W. A. Ellingson, S. A. Rothermel, and J. F. Simpson. "Nondestructive Characterization of Ceramic Composites Used as Combustor Liners in Advanced Gas Turbines." J. of Eng. for Gas Turbines and Power. Vol. 118, pp. 486-490 (July 1996).
7. W. A. Ellingson, J. G. Sun, K. L. More, and R. G. Hines. "Characterization of Melt-Infiltrated SiC/SiC Composite Liners Using Meso and Macro NDE Techniques." ASME Paper No. 2000-GT-0067, presented at 45th Gas Turbine and Aero Engine Symposium, Munich, Germany (May 2000).
8. J. G. Sun, T. E. Easler, A. Szweda, T. A. K. Pillai, C. Deemer, and W. A. Ellingson. "Thermal Imaging and Air-Coupled Ultrasound Characterization of a Continuous Fiber Ceramic Composite." Cer. Eng. and Sci. Proc. Vol. 20, No. 3, pp. 200-210 (1999).
9. J. Price, O. Jimenez, V. J. Parthasarthy, N. Miriyala, and D. Levoux. "Ceramic Stationary Gas Turbine Development Program: Seventh Annual Summary." ASM Paper No. 2000-GT-75, presented at Gas Turbine and Aero Engine Symposium, Munich, Germany (May 2000).
10. C. Deemer, J. G. Sun, and W. A. Ellingson. "One-Sided Thermal Imaging for Flaw Characterization of Ceramic Matrix Composites." Ceram. Trans. Vol. 124, pp. 23-240 (2001).

- 11 N. Miriyala, J. F. Simpson, V. J. Parthasarthy, and W. D. Brentnall. "The Evaluation of CFCC Liners after Field-Engine Testing in a Gas Turbine." Am. Soc. of Mech. Eng. Paper No. ASME 1999-GT-395 (1999).
12. M. Van Roode. "Ceramic Stationary Gas Turbine." Proc. of Adv. Gas Turbine Rev. Meeting, U.S. DOE Report DOE/OR-2048, pp. 633-657 (1997).